Multi-criticality and field induced non-BEC transition in frustrated magnets

Shouvik Sur[1], Yi Xu[1], Shuyi Li[1], Shou-Shu Gong[2], and Andriy H. Nevidomskyy[1]
[1]*Department of Physics and Astronomy, Rice University, Houston, TX 77005, USA and*
[2]*Department of Physics, Beihang University, Beijing 100191, China*

(Dated: May 31, 2023)

Frustrated spin-systems have traditionally proven challenging to understand, owing to the scarcity of controlled methods for their analyses. By contrast, under strong magnetic fields, certain aspects of spin systems admit simpler and universal description in terms of hardcore bosons. The bosonic formalism is anchored by the phenomenon of Bose-Einstein condensation (BEC), which has helped explain the behaviors of a wide range of magnetic compounds under applied magnetic fields. Here, we focus on the interplay between frustration and externally applied magnetic field to identify instances where the BEC paradigm is no longer applicable. As a representative example, we consider the antiferromagnetic $J_1-J_2-J_3$ model on the square lattice in the presence of a uniform external magnetic field, and demonstrate that the frustration-driven suppression of the Néel order leads to a Lifshitz transition for the hardcore bosons. In the vicinity of the Lifshitz point, the physics becomes unmoored from the BEC paradigm, and the behavior of the system, both at and below the saturation field, is controlled by a Lifshitz multicritical point. We obtain the resultant universal scaling behaviors, and provide strong evidence for the existence of a frustration and magnetic-field driven correlated bosonic liquid state along the entire phase boundary separating the Néel phase from other magnetically ordered states.

Introduction: Bose-Einstein condensates and superfluids are the most generic ground states of repulsively-interacting, dense Bose gases above one dimension [1]. For bosons hopping on a lattice, additional possibilities, such as Mott insulating phases, become possible at strong repulsive interactions [2]. It has been suggested that interacting bosons may exist in a symmetric liquid state – a Bose metal – in the presence of an extensively degenerate single-particle dispersion [3, 4]. The extensive-degeneracy not only constrains the phase space available for scatterings, but also enhances the low energy density of states. Over the past decade, the latter property has been utilized for stabilizing other kinds of Bose liquid states in Rashba spin-orbit coupled bosons [5], deconfined critical points between valence bond solids [6], superfluid phases in dipolar Bose-Hubbard model [7], certain tensor gauge theories [8], and fractonic superfluids [9]. In these systems, inter-boson interactions play a fundamental role in organizing the low energy behavior, which is in contrast to conventional Bose systems where the key mechanism, Bose-Einstein condensation (BEC), arises from quantum statistics. Unlike their fermionic counterparts, however, pure bosonic systems are comparatively rare in nature. It is therefore important to identify new platforms which may support unconventional phenomenology of bosonic systems.

Due to the connection between localized spins and bosons, frustrated magnets are promising candidates for realizing unconventional bosonic matter. Frustrated magnetic systems, however, pose significant challenges to a theorist, owing to a scarcity of controlled approaches, especially for low-spin systems [10, 11]. A rare avenue becomes available in the presence of a uniform magnetic field – since all spins in any quantum magnetic system will polarize when exposed to a sufficiently strong magnetic field, quantum fluctuations are suppressed in the vicinity of the resultant field-polarized (FP) state. In this region, the system can be mapped to a dilute gas of interacting bosons, and frustration manifests itself in the bosonic bandstructure. Indeed, much of the conventional phenomenology of interacting dilute Bose gases has been realized in such magnetic systems, including BEC, superfluidity, and Mott transition [12, 13]. Since the degree of frustration acts as an additional non-thermal tuning parameter, it introduces the possibility of realizing unconventional states of bosonic matter. Some such states, for example multi-Q condensates [14, 15] and multi-

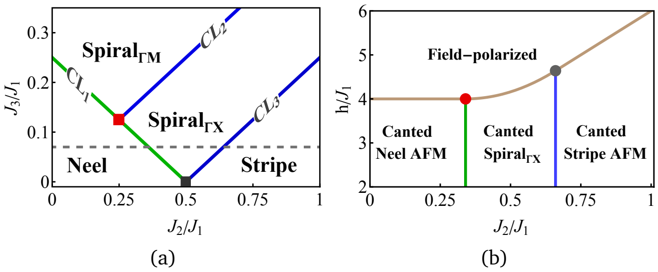

FIG. 1. Phase diagrams in the absence and presence of an externally applied magnetic field (h). (a) Classically, at $h=0$, the Néel antiferromagnet (AFM) phase at weak $J_{n>1}$ may continuously transition to spiral or stripe AFM phases along suitably chosen directions on the J_2-J_3 plane. Two multi-critical points exist at the intersections of critical lines (CL_n), marked by the (red) squares, at $(J_2, J_3) = (\frac{J_1}{4}, \frac{J_1}{8})$ and $(\frac{J_1}{2}, 0)$, respectively. (b) All magnetically ordered phases develop canting as a magnetic field is introduced, before transitioning to field-polarized states at sufficient high $h > h_c$. The brown curve denotes h_c/J_1 as a function of J_2/J_1, at a fixed J_3/J_1 [dashed line in (a)]. Multicritical points (filled circles) are obtained at the intersection of h_c and the boundaries between the magnetically ordered phases (vertical lines). The phase boundaries in (b) are obtained from a linear spin-wave analysis.

particle Bose condensates [16, 17], bear similarities to those proposed in spin-orbit coupled bosonic systems [18, 19]. Others, such as Bose metals, remain unexplored. Here, we focus on the vicinity of multicritical points that arise at the intersections of frustration-driven and magnetic-field-driven continuous transition lines. While frustration tends to stabilize quantum paramagnetic states, a high magnetic field nearly saturates the system. As we shall show, the combined effect of the two non-thermal agents facilitates a controlled access to Bose liquid states in frustrated magnets under an applied magnetic field.

The zero-temperature transition between an FP and magnetically ordered state is expected to be continuous, whereby the spin-rotational symmetry perpendicular to the field-polarization direction is spontaneously broken. In the bosonic language, it can be viewed as a density-driven transition between a trivial insulator with no particles to a superfluid [20]. On the superfluid side of the phase transition, the bosons usually develop an off-diagonal long range order (ODLRO), thus, undergoing a Bose-Einstein condensation (BEC) [1, 21]. The transition itself belongs to the 'BEC universality class', which is characterized by the dynamical critical exponent $z = 2$ [22]. Such magnetic-field tuned transitions are relevant to mainly two classes of spin systems, antiferromagnets and quantum paramagnets. Extensive experiments on both kinds of systems have established the importance of BEC-based perspective in understanding the physics of a wide variety of magnetic compounds under applied magnetic fields [23–40]. Here, we propose scenarios where this conventional outcome breaks down. In particular, we establish (i) transitions that go beyond the BEC universality class, and (ii) explore the possibility of emergent Bose metallic physics in spin systems exposed to strong magnetic fields.

Model and Phase diagram: We consider a spin-$\frac{1}{2}$ Heisenberg model on the square lattice with long range antiferromagnetic interactions,

$$H_0 = J_1 \sum_{\langle \boldsymbol{r}\boldsymbol{r}'\rangle} \vec{S}_{\boldsymbol{r}} \cdot \vec{S}_{\boldsymbol{r}'} + J_2 \sum_{\langle\langle \boldsymbol{r}\boldsymbol{r}'\rangle\rangle} \vec{S}_{\boldsymbol{r}} \cdot \vec{S}_{\boldsymbol{r}'} + J_3 \sum_{\langle\langle\langle \boldsymbol{r}\boldsymbol{r}'\rangle\rangle\rangle} \vec{S}_{\boldsymbol{r}} \cdot \vec{S}_{\boldsymbol{r}'} \tag{1}$$

where all $J_n > 0$, and $\vec{S}_{\boldsymbol{r}}$ represents the three-component spin-1/2 operator at site $\boldsymbol{r}$. It is convenient to employ J_1 as the overall energy scale, and define dimensionless ratios $\tilde{X} = X/J_1$ for any quantity X that possesses the dimension of energy. The classical phase diagram, obtained by analyzing the Luttinger-Tisza (LT) bands [41] is presented in Fig. 1a. For $\tilde{J}_2 + 2\tilde{J}_3 < 1/2$ a Néel antiferromagnet (AFM) is realized. In the complement of this region, classically, various spiral and stripe ordered phases are expected. Transitions between the Néel and other antiferromagnetically ordered phases manifest themselves as Lifshitz transitions of the LT band, where the nature of the dispersion about the band minimum changes qualitatively. The corresponding critical points lie along the line $\tilde{J}_2 + 2\tilde{J}_3 = 1/2$, henceforth labeled as 'critical line 1' (CL_1). Because of the enhanced density of states on CL_1, quantum fluctuations may be expected to suppress magnetic order in its vicinity [42–45]. Indeed, recent numerical simulations indicate the presence of quantum spin liquid and valence bond solid phases in the vicinity of CL_1 [46–48]. We note that two other critical lines are present in the phase diagram: CL_2 (CL_3) separates the two spiral-ordered (stripe-ordered and spiral ordered) phases. Here, we primarily focus on the impact of CL_1 on the phase diagram.

We introduce a uniform magnetic field, B, such that the system is governed by

$$H(h) = H_0 - h \sum_{\boldsymbol{r}} S^{(z)}_{\boldsymbol{r}}, \tag{2}$$

where $h := g\mu_B B$ is the Zeeman field with g and μ_B denoting the Landé g-factor and Bohr magneton, respectively. The magnetic field tends to polarize the spins along $\hat{z}$ direction, and cants the AFM order. At sufficiently high fields, the canted AFM phases give way to field polarized (FP) states, which are classical ground states with all spins polarized along the magnetic field direction (here, $\hat{z}$). A constant-$\tilde{J}_3$ slice of the resultant phase diagram is depicted in Fig. 1b. In this letter, we focus on the neighborhood of the transition between the canted AFM and FP phases. In particular, we ask how the transition is affected by the Lifshitz criticality along CL_1. We formulate the scaling theory for the multicritical points at the intersection of the saturation-field surface and CL_1 (see Fig. 1b), to show the existence of magnetic field-tuned transitions of novel, non-BEC niversality class for all points on CL_1. These non-BEC critical points strongly affect the phase diagram in their vicinity, most remarkably through the stabilization of a quantum liquid state at sub-critical fields.

Non-BEC transitions: The critical strength of the magnetic field necessary to drive the transition – the saturation field – will henceforth be called h_c. In the vicinity of h_c, spin fluctuations may be conveniently modeled by density and phase fluctuations of hardcore bosons, through the Matsubara-Matsuda transformation [49, 50],

$$S^{(+)}_{\boldsymbol{r}} \to b^\dagger_{\boldsymbol{r}}; \quad S^{(-)}_{\boldsymbol{r}} \to b_{\boldsymbol{r}}; \quad S^{(z)}_{\boldsymbol{r}} \to \frac{1}{2} - \rho_{\boldsymbol{r}}. \tag{3}$$

Thus, we rephrase the problem in terms of the hardcore bosons, $b_{\boldsymbol{r}}$, with $\rho_{\boldsymbol{r}}$ being their local density. The Hamiltonian acquires the form of a Bose-Hubbard model on the square lattice

$$H(h) = \int \frac{d^2K}{(2\pi)^2}[\mathscr{E}(\boldsymbol{K}) - \mu(h)] b(\boldsymbol{K})^\dagger b(\boldsymbol{K}) + \int \frac{d^2Q}{(2\pi)^2} V(\boldsymbol{Q})\rho(-\boldsymbol{Q})\rho(\boldsymbol{Q}) + U\sum_{\boldsymbol{r}} n_{\boldsymbol{r}}(n_{\boldsymbol{r}} - 1), \tag{4}$$

where the last term enforces the hardcore condition in the limit $U \to \infty$ [50]. The "chemical potential", $\mu(h) = \sum_{i=1}^{3} J_i - h$, is tuned by h, and it controls the average density of bosons. The dispersion, $\mathscr{E}(\boldsymbol{K})$, and the coupling function, $V(\boldsymbol{Q})$, are independent of h, but sensitive to the J_n's. In particular, $\mathscr{E}(\boldsymbol{K})$ tracks the LT band structure, and reflects the singularities at the classical phase boundaries: at a fixed $\tilde{J}_3$ and as a function of $\tilde{J}_2$, the boson band undergoes Lifshitz transitions as the critical lines are crossed. The existence of such a transition is directly diagnosed by the low-energy density of states, which acquires a more singular energy-scaling at a Lifshitz critical point than the abutting phases. We note that XXZ anisotropies, if present, can be absorbed in $V(\boldsymbol{Q})$.

In the Néel AFM phase the dispersion is minimized at the M-point of the BZ. Thus, the long wavelength fluctuations of the bosons, Φ, carry momenta in the vicinity of the M-point, and the low energy effective theory governing these fluctuations is given by $S_M = \int d\tau\, d\boldsymbol{r}\, \mathscr{L}_M[\Phi(\tau, \boldsymbol{r})]$ with

$$\mathscr{L}_M[\Phi] = \Phi^*[\partial_\tau + \varepsilon(\boldsymbol{\nabla}) - \mu_{\text{eff}}]\Phi + g|\Phi|^4, \tag{5}$$

where we have expanded the dispersion as $\mathscr{E}((\pi,\pi) + \boldsymbol{k}) = -\mathscr{E}_0 + \varepsilon(\boldsymbol{k})$ such that $\varepsilon(\boldsymbol{k}) \geq 0$, and defined the effective parameters $\mu_{\text{eff}} = h_c - h$ with $h_c = (3J_1 - J_2 - J_3)$, and $g := V(\boldsymbol{Q} = \boldsymbol{0}) = 2\sum_{i=1}^{3} J_i$. The magnetic field driven transition can be understood as a transition between a state with no bosons (an FP state; $\mu_{\text{eff}} < 0 \equiv h > h_c$) to a state with a finite density of bosons ($\mu_{\text{eff}} > 0 \equiv h < h_c$). The transition itself is described with respect to the critical point at $\mu_{\text{eff}} = 0 \equiv h = h_c$. If a magnetic long-range order is present for $h < h_c$, it is manifest as an ODLRO for the bosons with $\langle\Phi\rangle \neq 0$. As CL_1 is approached from the Néel AFM side of the phase diagram, does the field-driven transition continue to be described by the BEC universality class?

The dispersion about the band minimum in the vicinity of CL_1 takes the form

$$\frac{\varepsilon(\boldsymbol{k}, m_L)}{J_1} = m_L|\boldsymbol{k}|^2 + A\cos\gamma(k_x^4 + k_y^4) + 2A\sin\gamma\, k_x^2 k_y^2, \tag{6}$$

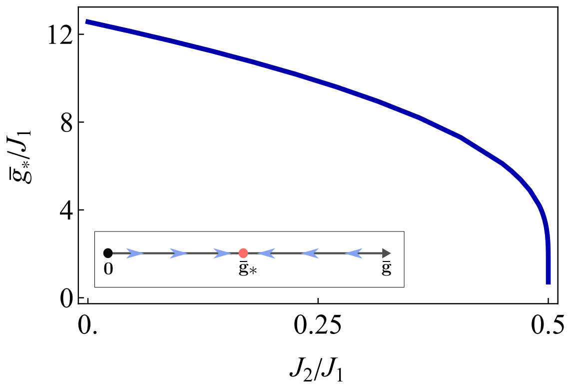

FIG. 2. Evolution of the fixed-point-interaction-strength at the Lifshitz multi-critical point along CL_1 [$\tilde{J}_3 = (1/2 - \tilde{J}_2)/2$]. Here, $\bar{g}_*$ is measured in units of $\epsilon = d - 4$ [see Eq. (8)]. (Inset) Schematic representation of the renormalization group flow for the dimensionless coupling $\bar{g}$. A non-trivial interacting fixed point is present for any $d < 4$.

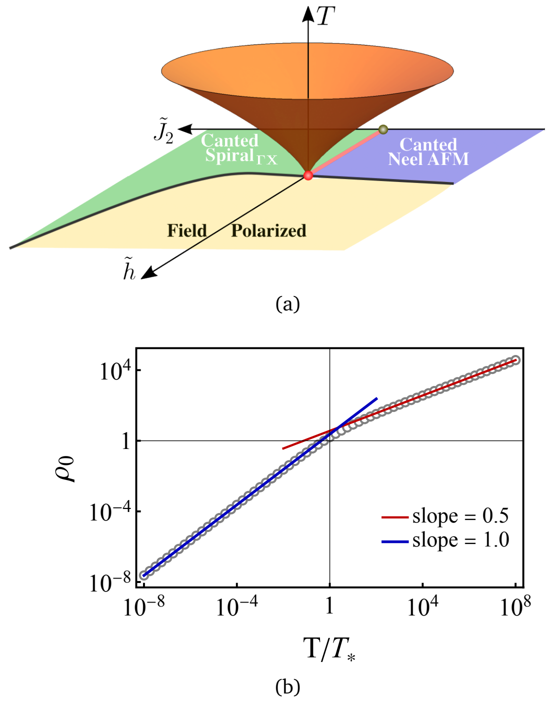

FIG. 3. (a) The multicritical point at the intersection of the field-polarized, canted-Néel, and canted-spiral phases controls the finite temperature (or frequency) behavior of the system over a wide energy window that lies within the (orange) critical cone. (b) Crossover behavior of ρ_0 as a function of temperature, determined by Eq. (9). The filled-circles represent numerically evaluated values of ρ_0 in appropriate units. The solid lines are fits to the data, whose unequal slopes indicate a crossover behavior associated with entering the critical-cone at sufficiently high-T. ♣ [Needs more explanation].

where the 'Lifshitz mass' $m_L = (1/2 - \tilde{J}_2 - 2\tilde{J}_3)$, and the parameters $A = \frac{1}{24}\sqrt{36\tilde{J}_2^2 + (2\tilde{J}_2 + 16\tilde{J}_3 - 1)^2}$ and $\gamma = \tan^{-1}\left\{6\tilde{J}_2/(2\tilde{J}_2 + 16\tilde{J}_3 - 1)\right\}$. In the parameter regime where $m_L > 0$, the field-driven transition belongs to the BEC class. As CL_1 is approached, $m_L \to 0$ and the field driven transition belongs to a distinct universality class that is controlled by the Lifshitz multi-criticality point (LMCP) at $h = h_c$ and $\tilde{J}_2 = \tilde{J}_{2,c}$. At the LMCP, the chemical potential $\mu = 0$, and, owing to the divergent DoS, strong quantum fluctuations arise in the presence of interactions among bosons. It is manifest in $V_{\rm eff}$ becoming strongly relevant at the Gaussian fixed point governed by the first term in Eq. (5). This strong coupling theory, however, is exactly solvable at $T = 0$, due to the absence of particle-hole excitations [20, 22]. In particular, the positive semi-definiteness of $\varepsilon(\boldsymbol{q})$ leads to a chirality-like constraint on the bosonic-dynamics, which protects the quadratic terms in the action against quantum corrections [51]. This is analogous to chiral fermionic liquids, where tree-level or classical critical exponents remain robust against quantum fluctuations, thanks to the chiral dynamics [52, 53]. Thus, in the present case, the tree-level critical exponents,

$$z = 4; \quad \nu_h = 1/4; \quad \nu_J = 1/2; \quad \eta = 0, \tag{7}$$

do not accrue anomalous dimensions through quantum fluctuations. Here, z is the dynamical critical exponent, ν_h and ν_J control the scaling of the correlation length along h and J_2 axes, respectively, and η is the anomalous dimension of Φ. Since this is a multi-critical point, the correlation length with respect to the LMCP is given by $\xi = 1/\sqrt{\xi_h^{-2} + \xi_J^{-2}}$ with $\xi_h \sim |h - h_c|^{-\nu_h}$ and $\xi_J \sim |J_2 - J_{2,c}|^{-\nu_J}$. The critical exponents imply the magnetic-field driven transition at $J_2 = J_{2c}$ does not belong to the BEC universality class, which is characterized by $\xi \sim |h - h_c|^{-1/2}$.

In contrast to the particle-hole channel, non-trivial quantum fluctuations are present in the particle-particle channel, which drives the system towards an interacting fixed point. To see this, we perform Wilsonian renormalization group (RG) analysis at $d = 4 - \epsilon$, where d is the number of spatial dimensions. We obtain the following one-loop RG flow of the parameters in $\mathscr{L}_M$:

$$\partial_\ell \bar{g} = \epsilon \bar{g} - \frac{f_g(\gamma)\, \bar{g}^2}{16\pi^2 J_1 A}, \quad \partial_\ell \bar{\mu} = 4\bar{\mu}, \quad \partial_\ell \bar{m}_L = 2\bar{m}_L, \tag{8}$$

where ℓ is the logarithmic length-scale, $(\bar{g}, \bar{\mu}, \bar{m}_L) = \left(\Lambda^{-\epsilon} g, \Lambda^{-4}\mu_{\rm eff}, \Lambda^{-2} m_L\right)$, Λ is the ultraviolet (UV) momentum cutoff, and $f_g(\gamma) = \int_0^1 \frac{dt}{\cos\gamma[t^2+(1-t)^2]+2\sin\gamma(1-t)t}$. Since the LMCP is a multicritical point, it has two independent relevant directions, $\bar{\mu}$ and $\bar{m}_L$. By maintaining multicriticality of the LMCP, i.e. setting the bare values $\bar{m} = 0 = \bar{\mu}$, we obtain a stable fixed point at $(\bar{g}_*, \bar{\mu}_*, \bar{m}_{L,*}) = \left(16\pi^2 J_1 A f_g^{-1}(\gamma)\epsilon, 0, 0\right)$. Extrapolating the result to $\epsilon = 2$, yields a fixed point coupling $\bar{g}_* = 32\pi^2 J_1 A f_g^{-1}(\gamma)$, which is independent of the UV structure of the interaction vertex, such as XXZ anisotropies. Because of its dependence on A and γ, $\bar{g}_*$ varies along CL_1, as shown in Fig. 2. In particular, as the critical point at $(A, \gamma) = (\frac{1}{8}, \frac{\pi}{2}) \equiv (\tilde{J}_2, \tilde{J}_3) = (\frac{1}{2}, 0)$ is approached along CL_1, $f_g(\gamma) \sim \ln\frac{1}{\pi/2-\gamma} \gg 1$; consequently, the fixed point is pushed to weaker couplings, and the one-loop result would appear to become more accurate as $\gamma \to \pi/2$.

Multicriticality and crossover behaviors: The LMCP is an example of 'zero-scale-factor universality', and the scaling functions for all observables are completely determined by microscopic or bare parameters [22]. Here, we focus on finite temperature properties within the multi-critical cone emanating from from the LMCP, as depicted in Fig. 3a. The shape of the cone is controlled by the temperature

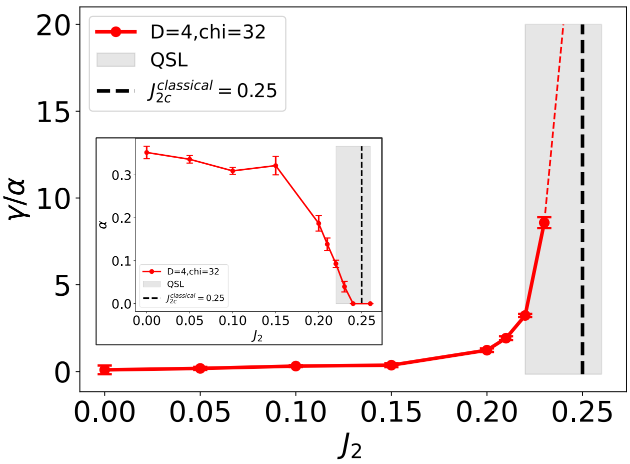

(a)

FIG. 4. Crossover in the scaling of $[1/2-\langle S^{(z)}\rangle]$ with $\Delta h := (h_c - h)$ as a function of increased frustration, obtained from iPEPS simulations. The data is fitted to the function, $[1/2-\langle S^{(z)}\rangle] = \alpha\Delta h \ln\frac{h_c}{\Delta h} + \gamma\sqrt{\Delta h}$. Deep in the Néel phase the transition would belong to the Bose-Einstein condensation universality class; consequently, $\alpha \sim 1$ (inset) and $\gamma \ll 1$. As the system is pushed towards the classical phase boundary, the ratio γ/α increases with $\alpha \to 0$. The shaded region indicates the regime over which a quantum spin liquid state has been reported at $h = 0$ [47]. The dashed line is an extrapolation of the data towards $\tilde{J}_{2c}$. Here, we have fixed $\tilde{J}_3 = 1/8$.

scale, $T_* = \sqrt{T_{*,h}^2 + T_{*,J}^2}$ with $T_{*,h} \sim \xi_h^{-z} \sim |h - h_c|$ and $T_{*,J} \sim \xi_J^{-z} \sim |J_2 - J_{2,c}|^2$. Although the density of bosons at $h = h_c(\tilde{J}_2)$ vanishes at $T = 0$, thermal fluctuations at $T > 0$ makes it finite. Therefore, we expect the magnetization at $T > 0$ would be suppressed below that in the FP state. Using a finite-T scaling analysis [22, 54], we estimate the average boson density to scale as [41]

$$\rho_0(T) \equiv \langle \rho(T)\rangle = T^{d/4}\, f_T(T_*/T), \tag{9}$$

where the dimensionless function has the limiting behavior, $\lim_{x\ll 1} f_T(x) = \mathcal{O}(1)$ and $\lim_{x\gg 1} f_T(x) \sim 1/\sqrt{x}$. At the LMCP in $d = 2$, only the former limiting behavior is applicable, and a $\sqrt{T}$-scaling is obtained. Away from the LMCP but along the BEC-transition line, $\rho_0(T)$ displays a crossover behavior. At low temperatures ($T \ll T_*$) the BEC critical points dictate the scaling and $\rho_0 \sim T$. At sufficiently high temperatures ($T \gg T_*$), however, the system enters the critical cone and $\rho_0 \sim \sqrt{T}$. This crossover behavior is depicted in Fig. 3b.

How does the LMCP affect the phase diagram at sub-critical fields? There are two primary degrees of freedom that control the behavior of the system at sub-critical fields, viz. density and phase fluctuations of the bosons. While a finite mean density reflects the deviation of $\langle S^{(z)}\rangle$ from 1/2, phase fluctuations determine the correlation between $S^{(+)}$ and $S^{(-)}$. First, we consider the asymptotic behavior of the mean density in the region $0 < (1 - h/h_c) \ll 1$, which corresponds to $0 < \mu_{\text{eff}} \ll J_1$. From one-loop RG analysis, we obtain the scaling of the mean density with μ_{eff} [41],

$$\rho_0(\mu_{\text{eff}}) = \mu_{\text{eff}}^{d/4}\, f_h\big(m_L^2/\mu_{\text{eff}}\big). \tag{10}$$

The dimensionless scaling function, $f_h(x)$, has the following limiting behavior, $\lim_{x\ll 1} f_h(x) = \mathcal{O}(1)$ and $\lim_{x\gg 1} f_h(x) \sim 1/\sqrt{x}$. Therefore, for a fixed μ_{eff}/J_1 at $d = 2$, as the system is tuned towards the LMCP from the canted Néel phase, the asymptotic scaling of $\rho_0 = [1/2 - \langle S^{(z)}\rangle]$ crosses over from $\rho_0 \sim (h_c - h) \to (h_c - h)^{1/2}$. We verify this crossover behavior through unbiased iPEPS calculations as demonstrated in Fig. 4.

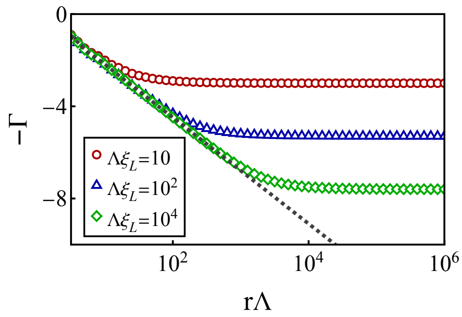

FIG. 5. Indications of a quantum critical point at sub-critical fields.

Emergent algebraic liquid: In order to understand the behavior of phase fluctuations at sub-critical fields within a unified framework, we introduce the hydrodynamic variables, ϑ and $\delta\rho$, which represent the long-wavelength phase and density fluctuations, respectively, of boson field, Φ, such that

$$\Phi(\tau, \boldsymbol{r}) = \sqrt{\rho_0 + \delta\rho(\tau, \boldsymbol{r})}\; e^{i\vartheta(\tau,\boldsymbol{r})}. \tag{11}$$

For $\tilde{J}_2 < \tilde{J}_{2,c}$ the FP state transitions into a canted Néel-AFM as h is lowered below h_c. This phenomenon is reflected in an $U(1)$ symmetry breaking transition for the bosons, whereby $\langle\Phi\rangle \sim \sqrt{\rho_0}e^{-\frac{1}{2}\langle\vartheta^2\rangle} \neq 0$, which implies existence of an off-diagonal long-range order (ODLRO), hence a BEC [1, 21]. As $\tilde{J}_2 \to \tilde{J}_{2c}$, the condensate fraction $\sim \langle\Phi\rangle$ is suppressed due to increased phase fluctuations. What is the fate of the system as $\langle\Phi\rangle \to 0$?

The dynamics of Φ, as dictated by S_M, is controlled by *two* independent length scales, $\rho_0^{-1/2}$ and m_L^{-1}. We fix the mean density ρ_0 (for fields $h < h_c$) and consider the influence of m_L (which controls proximity to CL_1) on the dynamics. We obtain an effective action for the phase fluctuations by submitting Eq. (11) to S_M, and integrating out $\delta\rho$ [41],

$$S_\vartheta = \int \mathrm{d}k \left[\frac{k_0^2}{4g} + \rho_0\varepsilon(\boldsymbol{k}, m_L)\right]\vartheta(-k)\vartheta(k). \tag{12}$$

Here, $\mathrm{d}k = \frac{dk_0 d\boldsymbol{k}}{(2\pi)^3}$, and we have dropped sub-dominant terms that do not affect the scaling behavior at the leading order, as detailed in the Supplemental Materials [41]. We note that the propagator of ϑ is non-perturbative in g, and the phase fluctuations disperse as $\sqrt{4g\rho_0\varepsilon(\boldsymbol{k}, m_L)}$, which is analogous to the dispersion of magnons in the canted Néel phase [41]. The long-wavelength behavior of the equal-time correlation function,

$$\langle S_{\boldsymbol{0}}^{(+)} S_{\boldsymbol{r}}^{(-)}\rangle \sim \langle\Phi^\dagger(0,\boldsymbol{0})\Phi(0,\boldsymbol{r})\rangle = \rho_0 \exp\{-\Gamma(\boldsymbol{r}, \xi_L)\}, \tag{13}$$

is determined by the correlation length $\xi_L \propto m_L^{-1/2}$ through $\Gamma(\boldsymbol{r}, \xi_L)$. The function $\Gamma(\boldsymbol{r}, \xi_J)$ is most easily computed along the line $16\tilde{J}_3 = 4\tilde{J}_2 + 1$, on which $\varepsilon(\boldsymbol{k}, m_L)$ acquires an C_∞-rotational symmetry and $\xi_L = \frac{1}{\Lambda}\sqrt{\frac{\tilde{J}_2}{6(1/4 - \tilde{J}_2)}}$ with Λ being the UV cutoff for S_ϑ. As shown in Fig. 5, for $|\boldsymbol{r}| \gg \xi_L$, $\langle S_{\boldsymbol{0}}^{(+)} S_{\boldsymbol{r}}^{(-)}\rangle$ saturates to a non-universal value (dependent on ρ_0 and ξ_L), implying the presence of ODLRO in Φ. We clearly observe a suppression of the condensate fraction as

CL_1 is approached (i.e. $\xi_L \to \infty$). In the opposite limit, a universal scaling is obtained, indicating the presence of a quantum critical point (QCP) as $\xi_L \to \infty$ (dashed line in Fig. 5). This putative QCP is characterized by the absence of an BEC, i.e. $\langle \Phi \rangle = 0$. At small but finite-T the canted Néel phase possess only a quasi-long range order, and goes through a Berezinskii-Kosterlitz-Thouless (BKT) transition upon raising T. Since the BKT transition scale, $T_{\rm BKT}$, is controlled by m_L, it is expected to be suppressed as CL_1 is approached. We note that these crossovers are not controlled by the multicritical cone in Fig. 3a, but the critical fan supported by the critical point at $m_L = 0 \equiv \tilde{J}_2 = \tilde{J}_{2c}$ for $h < h_c$ (see Fig. 1b).

The QCP indicated above realizes a higher-dimensional analog of the Luttinger liquid, where a condensate cannot form due to strong infrared fluctuations. All points on CL_1 host such algebraic liquid states, which are parameterized by the critical exponent $\mathscr{W}$ that controls the long-wavelength behavior of transverse spin correlations:

$$\langle S_{\mathbf{0}}^{(+)} S_{\mathbf{r}}^{(-)} \rangle \sim \rho_0 (|\mathbf{r}|\Lambda)^{-\mathscr{W}}. \tag{14}$$

We find the following expression: $\mathscr{W} = \frac{1}{2\pi}\sqrt{\frac{g/J_1}{\rho_0 a}}\, f_w(\gamma, \phi_r)$ for this exponent, with f_w being a dimensionless function. Since $\mathscr{W} \propto \rho_0^{-1/2}$, it scales as $\sim (h_c - h)^{-1/4}$ in the vicinity of the saturation field. Although $f_{\rm w}$ generally depends on the orientation, ϕ_r, of the position vector, $\mathbf{r} = |\mathbf{r}|(\cos\phi_r, \sin\phi_r)$, this dependence is found to be weak. While generic points on CL_1 possess a C_4 rotational symmetry, an C_∞ symmetry emerges at $\gamma = \pi/4$, where CL_1 and CL_2 intersect (red square in Fig. 1). The C_∞ critical point would be expected to control the high energy behavior in its vicinity, including that along CL_3 where a different kind of higher-dimensional Luttinger liquid is expected [4, 55].

Conclusion: Motivated by the ability of frustration to stabilize unconventional states of matter in quantum spin systems, here we studied its interplay with an applied magnetic field. With the help of the $J_1 - J_2 - J_3$ antiferromagnetic Heisenberg model, we demonstrated that frustration limits the validity of the BEC paradigm in describing the approach to saturation field. In particular, the phase transition between magnetically ordered and field-polarized states no longer belongs to the BEC universality class on the critical line CL_1, where frustration suppresses magnetic order.

At sub-critical fields, it is possible to realize bosonic quantum liquid states which are stabilized by a combination of frustration and high magnetic fields. These quantum liquids are higher-dimensional analogues of those found in the spin-1 Haldane chain [22] and 1D valence bond solids [56]. We note that mechanisms similar to that described here may be responsible for stabilizing the quantum spin liquid phase in the Kitaev honeycomb compass model in magnetic field along the [111] direction [57]. A detailed investigation into such possibilities is left to future works.

Acknowledgments : The authors thank Andrey Chubukov and Oleg Tchernyshyov for fruitful discussions. The analytical work performed by S.S. and A.H.N. was supported by the U.S. Department of Energy Computational Materials Sciences (CMS) program under Award Number DE-SC0020177. The numerical calculations performed by Y.X. were supported by the U.S. National Science Foundation Division of Materials Research under the Award DMR-1917511. The computing resources at Rice University were supported in part by the Big-Data Private-Cloud Research Cyberinfrastructure MRI-award funded by NSF under grant CNS-1338099 and by Rice University's Center for Research Computing (CRC). S.S.G. was supported by the NSFC (11874078).

[1] A. Leggett, Rev. Mod. Phys. **73**, 307 (2001).
[2] M. P. Fisher, P. B. Weichman, G. Grinstein, and D. S. Fisher, Phys. Rev. B **40**, 546 (1989).
[3] A. Paramekanti, L. Balents, and M. P. A. Fisher, Phys. Rev. B **66**, 054526 (2002), 0203171v1.
[4] S. Sur and K. Yang, Phys. Rev. B **100**, 024519 (2019).
[5] H. C. Po and Q. Zhou, Nat. Commun. **6**, 1 (2015).
[6] A. Vishwanath, L. Balents, and T. Senthil, Phys. Rev. B **69**, 224416 (2004).
[7] E. Lake, M. Hermele, and T. Senthil, Phys. Rev. B **106**, 064511 (2022).
[8] H. Ma and M. Pretko, Phys. Rev. B **98**, 125105 (2018).
[9] J.-K. Yuan, S. A. Chen, and P. Ye, Phys. Rev. Res. **2**, 023267 (2020).
[10] L. Balents, Nature **464**, 199 (2010).
[11] O. A. Starykh, Rep. Prog. Phys. **78**, 052502 (2015).
[12] T. Giamarchi, C. Rüegg, and O. Tchernyshyov, Nat. Phys. **4**, 198 (2008).
[13] V. Zapf, M. Jaime, and C. Batista, Rev. Mod. Phys. **86**, 563 (2014).
[14] Y. Kamiya and C. D. Batista, Phys. Rev. X **4**, 011023 (2014).
[15] Z. Wang, Y. Kamiya, A. H. Nevidomskyy, and C. D. Batista, Phys. Rev. Lett. **115**, 107201 (2015).
[16] L. Balents and O. A. Starykh, Phys. Rev. Lett. **116**, 177201 (2016).
[17] S. Jiang, J. Romhányi, S. R. White, M. E. Zhitomirsky, and A. L. Chernyshev, arXiv preprint arXiv:2209.00010 (2022).
[18] V. Galitski and I. B. Spielman, Nature **494**, 49 (2013).
[19] H. Zhai, Rep. Prog. Phys. **78**, 026001 (2015).
[20] S. Sachdev, *Quantum phase transitions* (Cambridge university press, 2011).
[21] O. Penrose and L. Onsager, Phys. Rev. **104**, 576 (1956).
[22] S. Sachdev, T. Senthil, and R. Shankar, Phys. Rev. B **50**, 258 (1994).
[23] H. Tanaka, A. Oosawa, T. Kato, H. Uekusa, Y. Ohashi, K. Kakurai, and A. Hoser, J. Phys. Soc. Jpn. **70**, 939 (2001).
[24] N. Cavadini, C. Rüegg, A. Furrer, H.-U. Güdel, K. Krämer, H. Mutka, and P. Vorderwisch, Phys. Rev. B **65**, 132415 (2002).
[25] R. Coldea, D. A. Tennant, K. Habicht, P. Smeibidl, C. Wolters, and Z. Tylczynski, Phys. Rev. Lett. **88**, 137203 (2002).
[26] M. Jaime, V. Correa, N. Harrison, C. Batista, N. Kawashima, Y. Kazuma, G. Jorge, R. Stern, I. Heinmaa, S. Zvyagin, *et al.*, Phys. Rev. Lett. **93**, 087203 (2004).
[27] A. Paduan-Filho, X. Gratens, and N. Oliveira Jr, Phys. Rev. B **69**, 020405 (2004).
[28] T. Waki, M. Kato, Y. Itoh, C. Michioka, K. Yoshimura, and T. Goto, J. Phys. Chem. Solids **66**, 1432 (2005).
[29] T. Nakajima, H. Mitamura, and Y. Ueda, J. Phys. Soc. Jpn. **75**, 054706 (2006).
[30] V. O. Garlea, A. Zheludev, T. Masuda, H. Manaka, L.-P. Regnault, E. Ressouche, B. Grenier, J.-H. Chung, Y. Qiu, K. Habicht, *et al.*, Phys. Rev. Lett. **98**, 167202 (2007).
[31] A. Kitada, Z. Hiroi, Y. Tsujimoto, T. Kitano, H. Kageyama, Y. Ajiro, and K. Yoshimura, J.Phys. Soc. Jpn. **76**, 093706 (2007).
[32] M. B. Stone, C. Broholm, D. H. Reich, P. Schiffer, O. Tchernyshyov, P. Vorderwisch, and N. Harrison, New J. Phys.

9, 31 (2007).
[33] V. O. Garlea, A. Zheludev, K. Habicht, M. Meissner, B. Grenier, L.-P. Regnault, and E. Ressouche, Phys. Rev. B **79**, 060404 (2009).
[34] A. A. Aczel, Y. Kohama, C. Marcenat, F. Weickert, M. Jaime, O. E. Ayala-Valenzuela, R. D. McDonald, S. D. Selesnic, H. A. Dabkowska, and G. M. Luke, Phys. Rev. Lett. **103**, 207203 (2009).
[35] A. A. Tsirlin, R. Nath, F. Weickert, Y. Skourski, C. Geibel, and H. Rosner, in *J. Phys. Conf. Ser.*, Vol. 145 (IOP Publishing, 2009) p. 012067.
[36] B. Thielemann, C. Rüegg, K. Kiefer, H. M. Rønnow, B. Normand, P. Bouillot, C. Kollath, E. Orignac, R. Citro, T. Giamarchi, *et al.*, Phys. Rev. B **79**, 020408 (2009).
[37] E. C. Samulon, Y. Kohama, R. D. McDonald, M. C. Shapiro, K. A. Al-Hassanieh, C. D. Batista, M. Jaime, and I. R. Fisher, Phys. Rev. Lett. **103**, 047202 (2009).
[38] I. Bostrem, V. Sinitsyn, A. Ovchinnikov, Y. Hosokoshi, and K. Inoue, J. Phys. Condens. Matter **22**, 036001 (2009).
[39] T. Hong, C. Stock, I. Cabrera, C. Broholm, Y. Qiu, J. B. Leao, S. J. Poulton, and J. R. D. Copley, Phys. Rev. B **82**, 184424 (2010).
[40] A. A. Tsirlin, R. Nath, J. Sichelschmidt, Y. Skourski, C. Geibel, and H. Rosner, Phys. Rev. B **83**, 144412 (2011).
[41] Please see 'Supplemetal Information' for more details.
[42] L. Capriotti and S. Sachdev, Phys. Rev. Lett. **93**, 257206 (2004).
[43] Y. A. Kharkov, J. Oitmaa, and O. P. Sushkov, Phys. Rev. B **98**, 144420 (2018).
[44] J. Reuther, P. Wölfle, R. Darradi, W. Brenig, M. Arlego, and J. Richter, Phys. Rev. B **83**, 064416 (2011).
[45] P. Sindzingre, N. Shannon, and T. Momoi, in *J. Phys.: Conference Series*, Vol. 200 (IOP Publishing, 2010) p. 022058.
[46] S.-S. Gong, W. Zhu, D. Sheng, O. I. Motrunich, and M. P. Fisher, Phys. Rev. Lett. **113**, 027201 (2014).
[47] W.-Y. Liu, J. Hasik, S.-S. Gong, D. Poilblanc, W.-Q. Chen, and Z.-C. Gu, Phys. Rev. X **12**, 031039 (2022).
[48] M. Wu, S.-S. Gong, D.-X. Yao, and H.-Q. Wu, Phys. Rev. B **106**, 125129 (2022).
[49] T. Matsubara and H. Matsuda, Prog. Theor. Phys. **16**, 569 (1956).
[50] E. G. Batyev and L. S. Braginskii, JETP **57**, 781 (1984).
[51] S. Sachdev, Z. Phys. B **94**, 469 (1994).
[52] X.-G. Wen, Phys. Rev. B **41**, 12838 (1990).
[53] S. Sur and S.-S. Lee, Phys. Rev. B **90**, 045121 (2014).
[54] D. S. Fisher and P. Hohenberg, Phys. Rev. B **37**, 4936 (1988).
[55] E. Lake, T. Senthil, and A. Vishwanath, Phys. Rev. B **104**, 014517 (2021).
[56] A. Iaizzi and A. W. Sandvik, in *J. Phys. Conf. Ser.*, Vol. 640 (IOP Publishing, 2015) p. 012043.
[57] N. D. Patel and N. Trivedi, Proc. Natl. Acad. Sci. U.S.A. **116**, 12199 (2019).